Measurement 293 (2027) 123670

Contents lists available at ScienceDirect

Measurement

journal homepage: www.elsevier.com/locate/measurement

Evaluation method for measuring mechanical impedance of the human hand-arm system under dynamic interaction forces

Simon Saurbier [a,*], Kai Wolter [a], Carina Spengler [a], Lukas Bunk [b], Jan-Heinrich Robens [a], Dieter Krause [b], Sven Matthiesen [a]

[a] Institute of Product Engineering, Karlsruhe Institute of Technology (KIT), Karlsruhe, 76131, Germany
[b] Institute of Product Development and Mechanical Engineering Design, TUHH Hamburg University of Technology, Hamburg, 21073, Germany

ARTICLE INFO

Keywords:
Hand-Arm Vibration
Mechanical Impedance
Dynamic Interaction Forces
Time-Resolved Impedance Analysis

ABSTRACT

This paper introduces a time-resolved evaluation method for determining the mechanical impedance of the human hand-arm system under time-varying force conditions within a single continuous test. The method is intended to support the investigation of dynamic hand-arm interaction conditions, while the present proof-of-concept focuses primarily on continuously varying applied grip-force profiles. Conventional impedance measurements, in contrast, are typically conducted at discrete constant force levels and require multiple separate tests at different force conditions. The proposed approach enables the measurement of mechanical impedance for continuously varying force profiles, resulting in increased test efficiency.

Experiments were conducted using a test rig compliant with DIN EN ISO 10819:2022. Test subjects were exposed to multi-sine translational vibration in z-direction at frequencies between 10 and 500 Hz, in accordance with DIN EN ISO 5349-1, while performing time-varying applied grip-force profiles. First, mechanical impedance was evaluated using an established frequency-dependent impedance evaluation method for constant force conditions as a reference. In a second step, the proposed time-resolved evaluation method was applied to determine mechanical impedance under non-stationary force conditions.

The results showed strong agreement between the dynamic method and the conventional approach, with a coefficient of determination of $R^2 = 0.9925$ over the investigated frequency range for static grip-force conditions. These findings indicate that mechanical impedance can be reliably calculated under time-varying force conditions, eliminating the need for separate measurements at each force level.

This method reduces experimental effort without compromising accuracy and enables future investigations of force-dependent, time-varying impedance behaviour of the human hand-arm system. Furthermore, it enables the representation of mechanical impedance as a time-resolved curve for different frequencies and varying interaction forces.

1. Introduction

Vibration exposure to the human body can lead to significant health impairments. The hand-arm system is particularly susceptible, as it plays a key role in transmitting force and information to technical systems that generate vibrations [1]. Research into the biomechanical effects of mechanical vibrations dates back to the 1970 s. Reynolds and Angevine demonstrated that vibration transmission to the hand-arm system elicits distinct physiological responses [2]. This topic remains highly relevant today, as the chronological overview of the transmission and effects of mechanical vibrations in the workplace by Cristea et al. clearly shows [3]. "*This review presents a contribution to vibration transmissibility studies involving hand–arm systems, providing and overview of research from 1980 to 2024, without assuming coverage of all relevant studies, as this field is extremely vast*" [3].

Handheld vibration-generating tools are one of the possible causes of work-related vibration exposure, and are particularly prevalent in industrial applications [4]. Examples include hammer drills, chipping hammers and chainsaw, which are used in various fields such as construction and forestry [3]. Due to the associated health risks, the use of such tools is subject to strict legal requirements within the European Union aimed at limiting exposure [5]. Excessive vibration exposure can

* Corresponding author.
E-mail address: simon.saurbier@kit.edu (S. Saurbier).

https://doi.org/10.1016/j.measurement.2026.123670
Received 2 May 2026; Received in revised form 22 September 2026; Accepted 22 October 2026
Available online 27 October 2026
0263-2241/© 2026 The Author(s). Published by Elsevier Ltd. This is an open access article under the CC BY license (http://creativecommons.org/licenses/by/4.0/).
Open access funding enabled and organized by Projekt DEAL.

cause health problems such as white finger syndrome, finger necrosis, retinal detachment and dizziness [6].

Various metrics are used to quantify the biomechanical stress on the hand-arm system. One such metric is the power absorbed by the hand-arm system ('vibration power absorption', VPA), as demonstrated by numerous studies [7–10]. There is also extensive literature on the vibration transmission of various tools and activities, summarized in Cristea et al. [3] and DIN EN ISO 22867:2022 [11], among others. Precise vibration transmission measurements are essential as they form the basis for any further analysis [12].

Basis for most of the metrics used is the mechanical impedance (MI). Which according to ISO 10068:2012–12 [13] is defined as the biodynamic response of the hand-arm system at the excitation point, expressed as the complex ratio between the excited force and the resulting velocity. Current research shows that MI is influenced by factors including coupling forces, arm posture and the experience of test subjects [14–16]. This paper focuses on coupling forces, consisting of grip and push forces. Furthermore, in real-world applications such as hammer drilling, the coupling force is not constant. Instead, dynamic, time-varying force curves occur [17].

The influence of push force has been investigated several times previously. For instance, Lindenmann et al. [1] evaluated the data from Jahn [18] and found that higher push forces led to lower vibration levels measured at the power-tool housing.. However, in another study, Uhl et al. [19] found that higher push forces can increase vibrations at the main tool handle. The influence of grip force has also been extensively documented [1]. Welcome et al. [20] define grip force as the necessary counterforce for guiding the tool, which significantly influences system dynamics and vibration perception [1,12]. The relationship between static grip forces and MIis well documented [21–24]. Biodynamic responses have also been investigated during continuously time varying grip-force conditions. Pan et al. [25] instructed participants to increase their applied grip force approximately linearly while vibration transmissibility was evaluated as a continuous function of grip force at discrete sinusoidal excitation frequencies. In a separate experiment, apparent mass and MI were determined under several discrete constant grip-force and combined grip-and-push-force conditions. Therefore, previous research has demonstrated the continuous acquisition and evaluation of force-dependent biodynamic responses, but it has not provided a time-resolved evaluation of MI across a broad frequency range during the same continuous measurement with varying applied grip force. Since forces while using a power-tool are not static and knowledge about the MI dependency to non-static forces is missing, the present study focuses on time based varying grip forces.

Until now, the influence on the MI of grip and push forces have predominantly been examined statically on shaker based test benches. The interface between tool and human is provided by standardised measuring handles in accordance with DIN EN ISO 10819-2021 [26]; the influence of the handle of these can be calibrated according to Heyden et al. [27]. Current studies specify the coupling forces statically and require them to remain constant throughout the measurement (e.g. [28], with a grip force of 30 N and a push force of 50 N, with a tolerance of ± 5 N). ISO 10068:2012–12 [13] documents validated evaluation methods for determining MI in these static conditions. Spengler et al. [10] recently conducted a large-scale investigation of MI over a large number of static combinations of different grip and push forces, taking 1500 measurements. All these investigations and measurements require separate static measurements for each combination of push and grip force, which is an extremely time-consuming process. Although test subjects can follow these dynamic force curves using the measuring handle [17]. Furthermore, signal segmentation, short-time frequency-domain evaluation and overlapping-window processing are established signal-processing approaches [29]. However, these established processing elements have not yet been integrated into an evaluation method that repeatedly determines the frequency-dependent MI of the hand-arm system over time during a single measurement with continuously varying applied interaction forces. The contribution of the present work is therefore not the introduction of segmentation or overlapping windows as new signal-processing techniques, but their systematic application and adaptation to the time-resolved calculation of hand-arm MI. The resulting method is intended to support both continuously varying force profiles and future investigations involving more complex dynamic interaction conditions.

Therefore, current research lacks a documented method for evaluating the MI of the hand-arm system repeatedly as a function of frequency and time during a single continuous measurement with time-varying applied interaction forces. This gives rise to the following research question for this work:

Main research question:

How can the dynamic behaviour of mechanical impedance be calculated on varying interaction forces?

To address this research question, a user study was conducted in which exploratory measurement data were collected. Measurements were performed under static grip and push force conditions as well as under dynamically varying interaction forces. To evaluate the static data, “Reference method” was used, as described in Chapter 2.5 and in line with the current state of research, representing an interpretation of ISO 10068:2012 [13]. For the dynamic data, a new evaluation method called DTIA (Dynamic Time-Resolved MI Analysis) was developed by combining the established mechanical-impedance calculation with signal segmentation and overlapping evaluation windows (see Chapter 3). The DTIA method was subsequently validated by comparison with the established method.

2. Experimental Framework

All experiments were conducted on the human–machine interaction test rig at the Institute of Product Engineering at the Karlsruhe Institute of Technology [1]. This setup, shown in Fig. 1 follows the methodologies established in previous MI research [30].

The test setup consists of two electromechanical shakers and a measuring handle designed in accordance with the ISO standard ISO 10068:2012–12 [13]. For this study, only the axial shaker (M124M, 10 kN; ETS Solutions Europe GmbH, Loffenau, Germany) was used. The secondary shaker (L215M, 2 kN force, ETS Solutions Europe, GmbH, Loffenau, Germany), which is typically used for rotational excitation via a rack-and-pinion system, was left inactive.

To measure the grip and push forces as well as the accelerations on the participant, a standardized measurement handle, compliant with DIN EN ISO 10819-2021 [26] was rigidly mounted on the shaker axis (Fig. 1).

The handle has a diameter of 40 mm. The design of the measuring handle is consistent with the description provided in Lindenmann's study [29]. The handle was calibrated according to the procedure proposed by Heyden et al. [27], which is an advancement to the methodology of Dong et al. [31] for the calibration of hand-arm vibration measurement systems. For this purpose, calibration masses of 0.159 kg and 0.309 kg were attached to the handle and the frequency-dependent calibration function was determined from apparent mass measurements. Lindenmann et al. [29] have previously reported on the dynamic characteristics and calibration of this measurement handle. The reported measurement error was below 3% across the investigated frequency range, except at 50 Hz where an error of 7% was observed. Furthermore, a finite element modal analysis of the handle conducted by Lindenmann et al. identified the first translational eigenfrequency at approximately 1320 Hz, which is substantially higher than the frequency range investigated in the present study. The corresponding calibration results are presented in Lindenmann et al. [30].

Fig. 2 shows Lindenmann's design and calibration of the measuring handle.

The instrumentation included:



Fig. 1. The left panel shows the visual force-tracking display presented to the participant, indicating the prescribed grip-force profile to be followed over time. The right panel shows the user-interaction test rig at the Karlsruhe Institute of Technology, with the participant adopting the standardized posture and interacting with the shaker system through an ISO-compliant instrumented handle while applying the prescribed time-varying grip force.

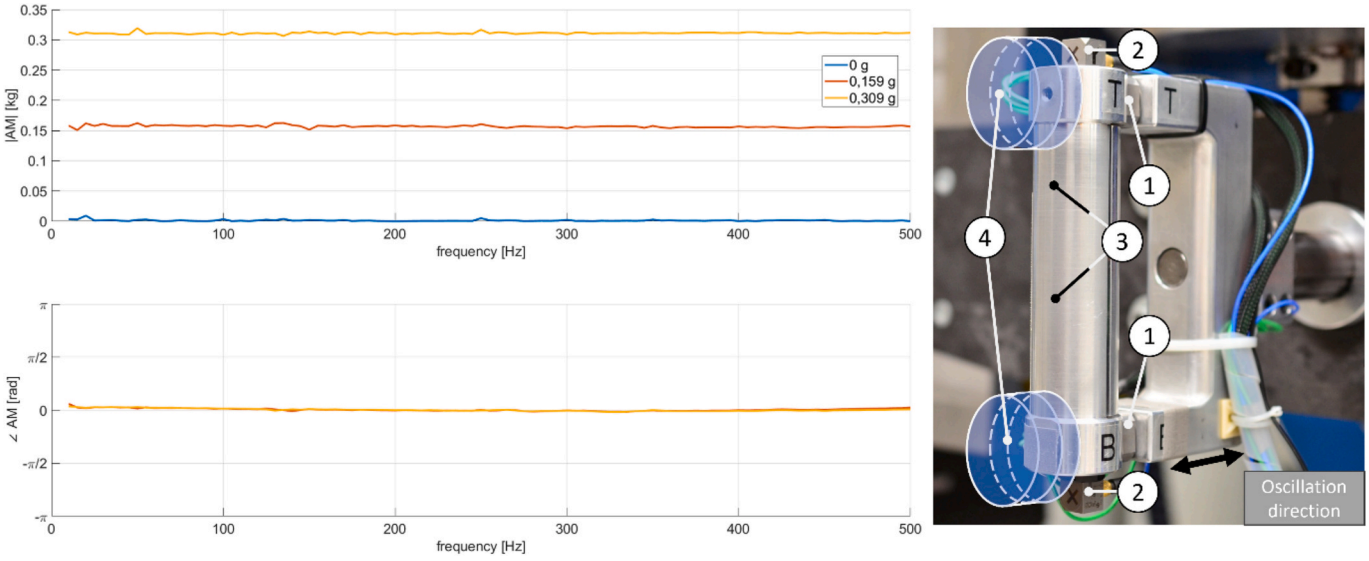


Fig. 2. Instrumented handle used in the present study. The handle design is based on the measurement handle proposed by Lindenmann et al. [30] and complies with the relevant ISO specifications. The handle is equipped with two accelerometers mounted at the upper and lower sections of the cylindrical handle, two triaxial force transducers (1) for measuring the interaction forces, and two grip-force sensors (3) integrated into the handle shells. The handle was calibrated according to the procedure proposed by Heyden et al. [27], using the calibration masses (4).

- Acceleration measurement sensor (2) in Fig. 2: two uniaxial accelerometers (type 356A15, PCB Piezotronics GmbH, Hückelhoven, Germany), which were mounted at the top and bottom of the cylindrical handle to capture translational acceleration.
- Grip force measurement sensor (3) in Fig. 2: Two uniaxial force sensors (type 9011A, [9]Kistler Instruments, Winterthur, Switzerland) were integrated within the split cylindrical handle.
- Push force measurement sensor (1) in Fig. 2.: Two triaxial force sensors (type 9027C, Kistler Instruments AG, Winterthur, Switzerland), which were mounted at the interface between the hand and the handle.

The dynamic signal path used to calculate apparent mass and MI comprises the axial force signals measured by the two triaxial force push force sensors and the acceleration signals measured at the handle. The grip-force sensors integrated into the handle shells are used exclusively to determine the applied grip force and associate each evaluation window with its corresponding grip-force condition. These dynamic signals are not used in the calculation of apparent mass or MI. A real-time data acquisition system (ADwin Pro II, Jaeger Computergesteuerte Messtechnik GmbH, Lorsch, Germany) recorded all signals. The signals from the upper and lower sensors were corrected for their mean offset. The force signals were summed, while the acceleration signals were combined by calculating the arithmetic mean of the respective sensor measurements. To minimize potential offset drift of the force measurement system, the instrumented handle was reset and zeroed before each measurement run. This procedure ensured a stable reference level throughout the experiments. The conducted measurements are sampled with 10 kHz which leads to a frequency resolution of 0.1 Hz per second measuring time. In combination with the used frequency step of 5 Hz for the multi-sine.

2.1. Test subjects

Twenty-five test subjects participated in the experimental study. Prior to data collection, all subjects completed standardized training to ensure the reproducibility of the force-tracking tasks. Participation was voluntary and the subjects were permitted to pause or terminate the experiment at any time; however, no interruptions occurred. The test rig was adjusted to ensure a consistent elbow flexion angle of 90°, in line with ISO 10068:2012–12 [13].

2.2. Excitation signal and calibration

The translational shaker operated within a multi-sine signal based on the 10–500 Hz frequency range, as defined by the upper limit in ISO 10068:2012–12 [13]. The use of a multi-sine signal was used to ensure comparability between different measurements [30]. To ensure maximal comparability between measurements the shaker was calibrated for each measurement day to a multi-sine from 10 Hz to 500 Hz in 5 Hz steps. The resulting time domain and frequency domain signals are illustrated in Fig. 3. The excitation signal was adjusted iteratively until the deviation between the target and actual amplitude was minimized. As seen in the time-based signal the multi-sine signal is repeating every 0.2 s, with each repetition showing the exact same form. The frequency domain shows well defined amplitudes for each 5 Hz step and nearly no signals in between.

2.3. Experimental procedure

The experimental procedure and measurement data were published at the VDI-Schwingungen [VDI conference Vibrations], focusing on the deviation of the measurement data from the specified grip profiles [32]. The exact procedure can be found in Saurbier's publication. This study only presents the most important steps [31].

All test subjects performed the same measurement tasks in randomized order. This followed the test procedure described by [32]. The subjects stood in a shoulder-width stance, as specified in ISO 10068:2012 [13].

The test plan included four predefined grip force profiles:

$$StaticValue : F_{Grip}(t) = 40N \tag{1}$$

$$Linear : F_{Grip}(t) = t^{*}8\frac{N}{s} \tag{2}$$

$$SineCurve : F_{Grip}(t) = 40^{*}\sin\left(t^{*}\frac{1}{s}\right) + 50N \tag{3}$$

a realistic, dynamic profile obtained from hammer drilling applications [32]This study used a dataset comprising two different experimental subsets. Static Value, Sine Curve and dynamic profile measurements were available from two participants, with three repeated measurements per participant. Linearly increasing grip force measurements were available from 25 participants, including the two, with three repeated measurements per participant. Thus, the dynamic dataset comprises 75 individual measurement runs. All force profiles were randomized. During measurement, the axial shaker generated vibrations in the translational direction along the test subjects' forearm axis according to DIN EN ISO 5349 [33]. Similar to the experimental procedure reported by Pan et al. [25], the grip force was continuously increased during the measurement, whereas no predefined push force was specified. Consequently, variations in push force were not part of the investigated experimental factors but resulted from the natural interaction of the subjects with the instrumented handle. The focus of the present study was therefore solely on the effect of time-varying grip force conditions

Accuracy was assessed in Saurbier's publication using the root mean square error (RMSE). For the profile derived from boreholes, the maximum RMSE observed was 13.10 N [32].

3. [34] Reference Evaluation Method

The current state of research outlines how to calculate MI in DIN ISO 10068:2012 [13]. This section outlines the method published by Lindenmann et al., which uses this standard and provides additional steps for determining MI [30]. According to this method, all static measurements were processed using the “ReferenceReference method” to evaluate MI. The multi-step procedure was performed in MATLAB (The MathWorks, Inc., USA). The individual steps of the method include the following activities:

Data Import and Preprocessing:

The recorded force signals were checked for deviations from the target values. Following Lindenmann et al. [30], recordings exceeding a 12% deviation threshold were discarded.

Fourier transformation & peak identification:

The time-domain force and acceleration signals were converted to the frequency domain using a discrete Fourier transform. The peak force and acceleration amplitudes were determined at the excitation frequencies.

Mechanical impedance Calculation:

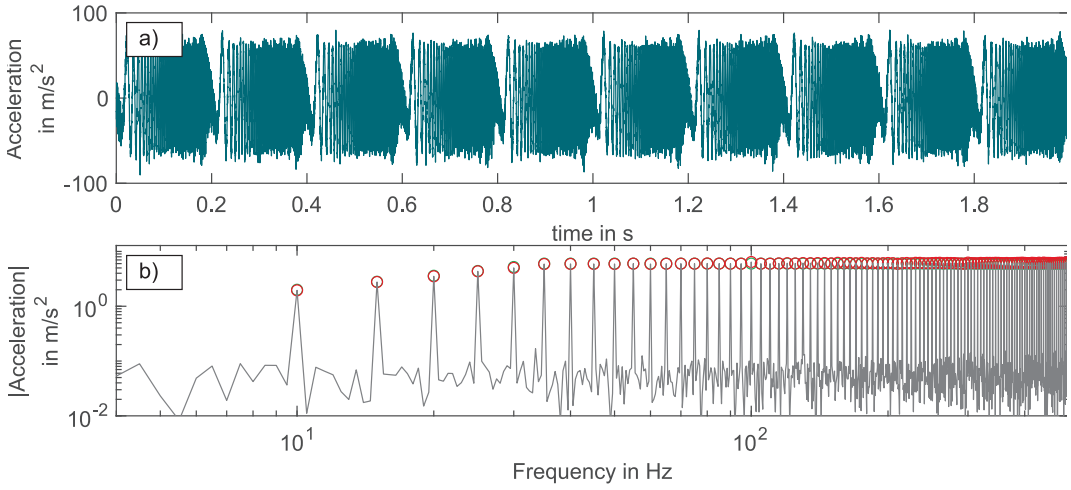


Fig. 3. Calibration of the shaker system. **Top a:** Representation of the raw signal over time for the multi-sine from 10 to 500 Hz. **Bottom b:** The specified amplitude is displayed as a ramp. Green dots indicate the target, red dots indicate the measured signal. The measured amplitude for the multi-sine wave is displayed in black.

The apparent mass (AM) was calculated as a complex ratio of force to acceleration. The theoretical MIwas derived by integrating the acceleration term using Fourier transformation (force divided by velocity). Compensation and calibration of the handle mass according to Heyden et al. [27] was applied to all data sets. Finally, each MI (Formular 4) value was associated with the corresponding test conditions (grip force, push force, and posture). The MI is determined at the excitation point, the hand–handle interface, and represents the dynamic response of the coupled hand–arm system at the driving point.

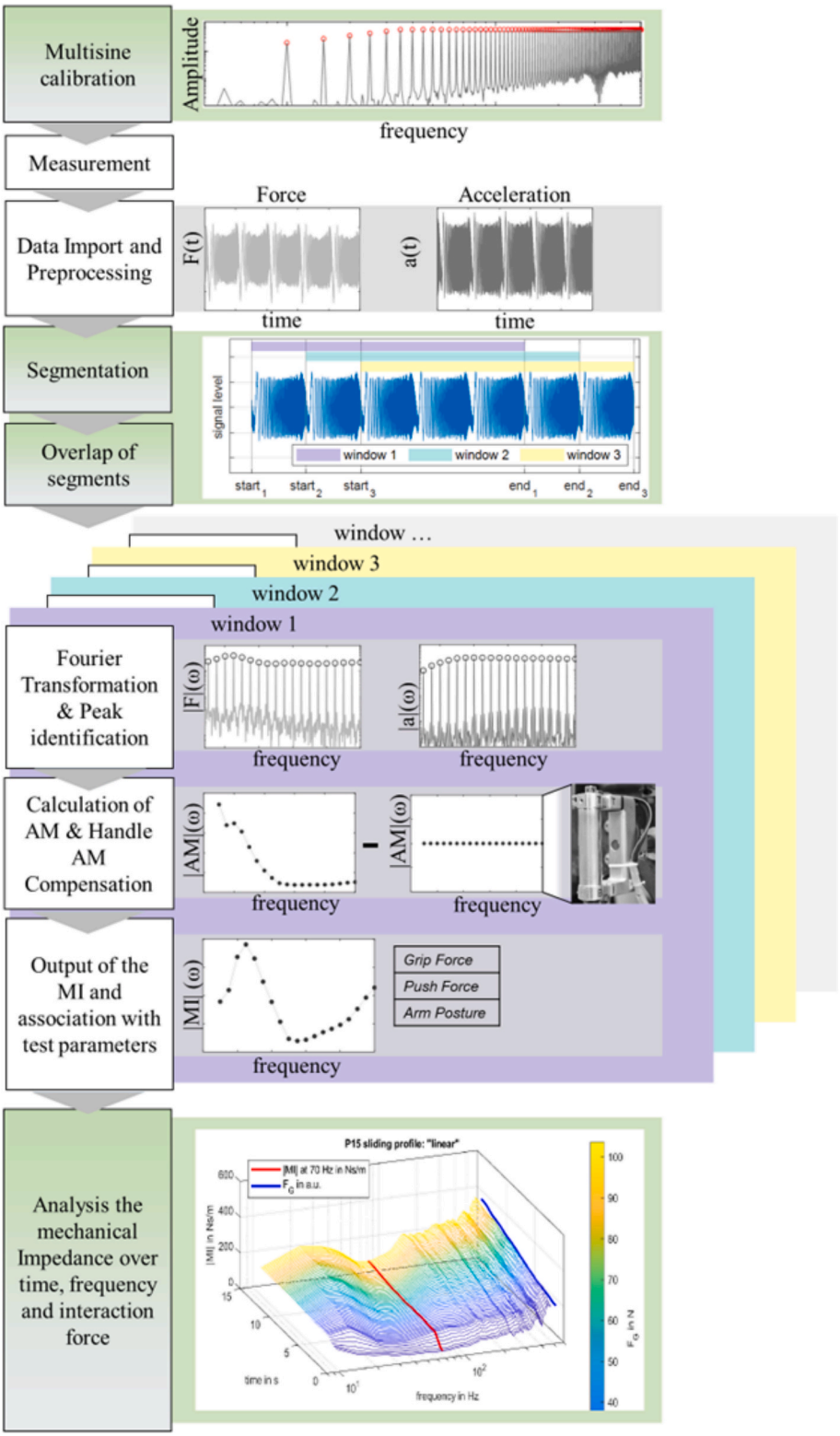


Fig. 4. Overview of the proposed Dynamic Time-Resolved mechanical Impedance Analysis (DTIA) method for evaluating mechanical impedance under dynamic interaction forces. The method extends"Reference"impedance evaluation procedure [21] by introducing three additional steps for excitation signal calibration, data segmenting and an overlapping analysis to enable time-resolved impedance evaluation.

$$MI(\omega) = \frac{F(i\omega)}{\dot{X}(i\omega)} = Re[MI(\omega)] + j^{*}Im[MI(\omega)] \quad (4)$$

4. DTIA – Dynamic Time-Resolved mechanical impedance analysis

The newly introduced DTIA method allows dynamic MI curves to be calculated over time and frequency, depending on dynamic interaction forces. It is based on the "Reference method" presented by Lindenmann et al. [30] in Chapter 2.5 under 'State of Research'.

The method presented in this paper is based on "Reference method"[30] and is visualized in Fig. 4. The green-highlighted boxes are added steps and are described in detail in the following section. Three additional evaluation steps are required prior to the FFT calculation. As shown in Fig. 4, the FFT and peak identification steps, the calculation of Am and Handle Am Compression, and finally the Output MI are now performed for each window. This sequence is not explained again here but can be found in Chapter 2.5. The calibration of the multi–sine excitation, already detailed in the Methods section, is not repeated here.

Segmentation:

Based on the repeating multi-sine with a period of 0.2 s the total measurement can be segmented into several subsets. Based on the total measurement time of 13 s, a total of 63 segments can be generated. Since the FFT over a segment length of 0.2 s has a limited frequency resolution the method developed, combines five segments into one evaluation step. This definition ensures that each segment contains enough cycles to enable stable frequency-based evaluation while maintaining sufficient temporal resolution. For each evaluation step a separate MI can be calculated.

Overlap of segments:

To increase the time resolution of the grip and push forces for one evaluation step of the calculated MI, a sliding window approach is used. Each evaluation step has an overlap with the previous step. The overlap was chosen to four multi-sine periods, which leads to the highest possible time resolution. This overlap allows the existing measurement data to be used more efficiently, improves the smoothing and stability of the resulting impedance curves, and increases the coherence of the calculated frequency components. This approach also reduces sensitivity to local measurement disturbances and enables a more consistent temporal representation of the MI under dynamic force conditions.In the following steps, the MI is determined for each individual segment using the "Reference method". By dividing the structure into segments, the MI can also be determined for forces that change over time.

4.1. Output of the new evaluation method

The developed method determines the MI under dynamic force conditions by segmenting the measurement signal and evaluating the segments in an overlapping manner. This allows a separate frequency-dependent impedance curve to be calculated for time varying interaction force in the measurement. Together, the resulting impedance curves form a continuously resolved force-frequency space that allows the force-dependent behavior to be represented across a wider range of operating conditions than in conventional static approaches.

In two-dimensional space, this higher resolution can be represented as a bundle of several impedance curves over the frequency, with each curve corresponding to a specific force combination. As an extension, a three-dimensional representation has been introduced: by adding time as a third axis, the time-based variation of the interaction force and the resulting changes in MI can be visualized simultaneously. This 3D representation allows the non–stationary behavior of the hand–arm system to be visualized across time, frequency, and interaction force.

5. Validation and dynamic evaluation

The results of this study are presented in two consecutive parts.

This section begins with an evaluation of the data recorded in this study under constant force conditions. This involves systematically comparing the established evaluation "Reference method" [29] with the dynamic method presented in this study. The objective is to ascertain the degree of agreement between the two methods under stationary conditions and whether the new method can reproduce the reference results.

The new method is applied to measurement data with time-varying grip forces in the concluding section. The linear force curve from section 2.3 was selected for exemplary representation as it exhibits clear and unambiguous variation over time. The other force curves examined, including sine profiles and application-based profiles, are documented in the appendix II & III.

5.1. Validation

To validate the new DTIA method introduced in Chapter 4, the mechanical impedance obtained using DTIA was compared with the reference evaluation method results described in Chapter 3. Validation was performed in two consecutive steps.

First, a static measurement of one participant was evaluated using both methods. This measurement was taken for the constant value F (t) = 40 N, which the participant could maintain with an error value of 0.81 N [32]. Based on the reference method, the participant applied mean push and grip forces of 9.9 N and 40.2 N, respectively. Since the complete measurement is evaluated as a single dataset, the reference evaluation yields one MI curve over frequency, shown in red in Fig. 5a.

The same measurement was also evaluated using the DTIA method. Due to its sliding-window evaluation, the DTIA method yields multiple MI curves, as the grip and push forces cannot be maintained at exactly the same level throughout the entire measurement. The area of all the resulting MI curves is highlighted in grey in Fig. 5a. From these curves, the DTIA curve with grip and push forces closest to the static reference condition was identified and is shown in blue. The best-fitting window was defined as the time window for which the sum of the absolute deviations of the grip and push forces from the corresponding static reference forces was minimal.

In addition, the 75 dynamic measurements, which increased linearly, from 25 participants (including the participant used for the preceding static comparison) were evaluated using the DTIA method. For each measurement, the time window in which the grip and push forces were closest to the static reference condition within ± 5N was selected. These force-matched time windows are shown in Fig. 5c and are predominantly located between approximately 4 and 6 s. This interval corresponds to the section of the linearly increasing grip-force profile in which the dynamically applied interaction forces most closely approach the static reference condition. Only the force-matched DTIA evaluation window was included for each of the 75 measurements. The resulting MI curves are shown as the blue area in Fig. 5a and were compared with the red static reference curve.

In the second evaluation step, two measurements were analysed for the same participant: one with a constant grip and push force (Static Value), and one with a grip-force curve that increased linearly (Linear Value). The static measurement was processed using the reference evaluation method, and the resulting MI curve is shown in red in Fig. 6. For the linear measurement, the DTIA method was applied to the entire measurement. The grip force increased evenly from 0 N to 100 N throughout the measurement period, while the push force remained at approximately 0 N. The grey area in Fig. 6a comprises all the MI curves resulting from the DTIA evaluation of this complete dynamic measurement.

From these curves, the impedance curve with force conditions most similar to the constant reference measurement was identified and is shown in blue. In this case, it corresponds to a segment with interaction

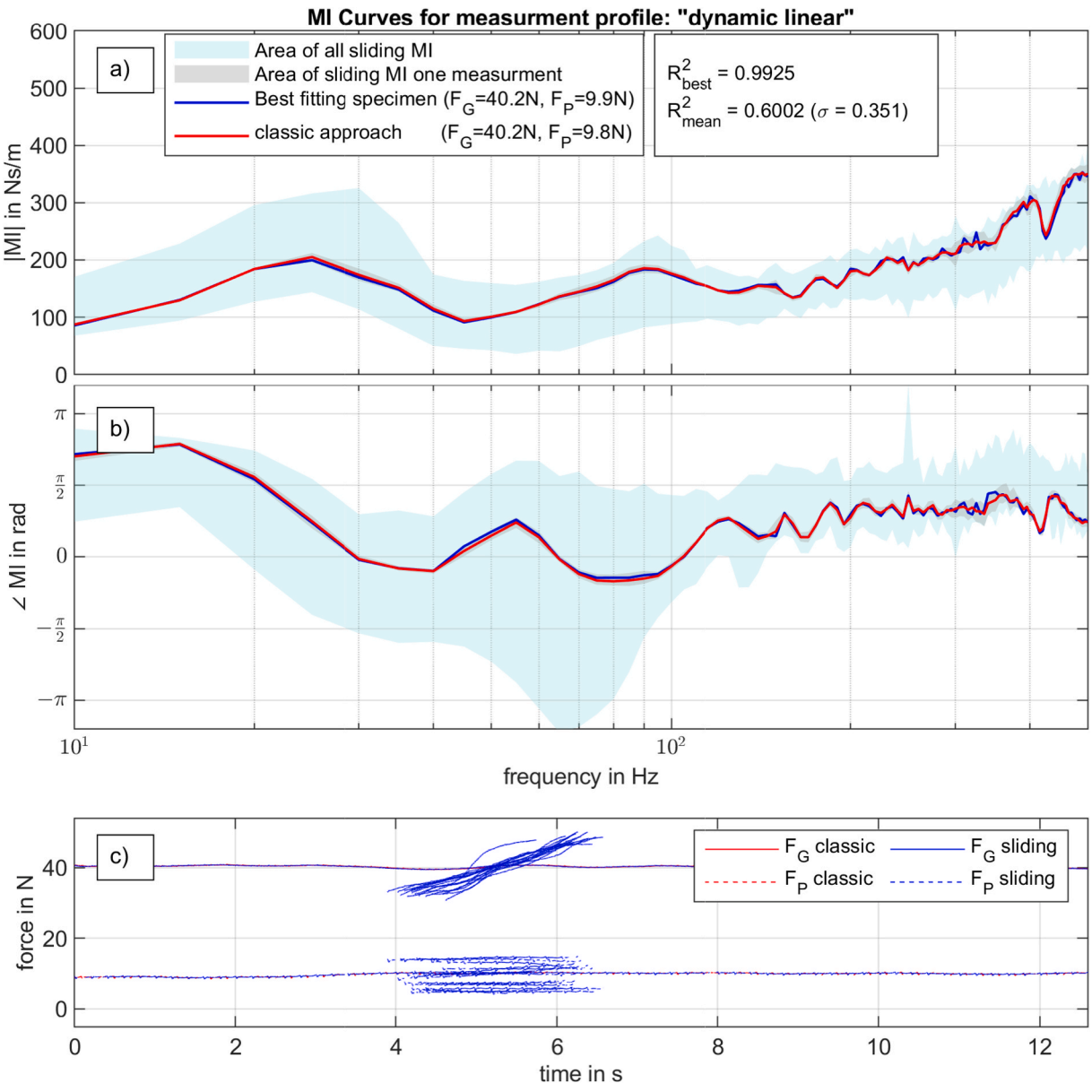


Fig. 5. Top a: 2D display of the mechanical impedance for static forces over a frequency range of 10 to 500 Hz. The mechanical impedance, as determined by the "Reference method", is shown in red and represents the reference [21]. The area of all the MI curves from the new DTIA method is highlighted in grey. The curve from the new DTIA method that most closely matches the grip and push forces of the static approach is shown in blue. The correlation between the blue and red curves is R^2 of 0.9925. The blue area represents the force-matched DTIA results from the 75 linearly increasing measurements; across these comparisons,($R_{mean}^2 = 0.6002$ &SD = 0.351). Middle b: The Phase from the mechanical Impedance in rad over the frequency. Bottom c: The grip and push force for static forces in Newtons over time. The continuous curves represent the static reference condition, while the clustered dynamic sections around approximately 4 s represent the individually selected force-matched windows from the 75 dynamic measurements.

forces of 39.9 N grip force and almost 0 N push force. Finally, the complete, linearly increasing force profiles of all 75 dynamic measurements from the 25 participants were evaluated using DTIA, without restricting the analysis to a force-matched window. The resulting MI curves, shown as the blue area in Fig. 6a, cover the full grip-force range occurring during the measurements, from 0 N to 100 N. [30,32]To determine the *best-fitting specimen*, the difference between the instantaneous grip and push forces of the dynamic measurement and the corresponding static reference forces was calculated for each time window. The *best-fitting specimen* was defined as the time window for which the sum of the absolute deviations of both force components was minimal:

$$\underset{i}{\operatorname{argmin}}\left(\left|F_{Gclassic} - F_{Gsliding}\right| + \left|F_{Pclassic} - F_{Psliding}\right|\right) \quad (5)$$

In the upper of Fig. 5, the MI for the evaluation method according to the established method is shown in red. A first peak between 20 and 30 Hz with 200 Ns/m can be seen. A second local peak is visible at 100 Hz with 180 Ns/m. From 150 Hz onwards, the MI rises continuously, with a global maximum at 500 Hz and a MI of 350 Ns/m. Since the new method leads to an overall of 65 MI curves there is no one single curve that can be shown. Instead, the Area of all MI curves is highlighted in grey and a single curve with the closest match in both grip and push force is shown in blue. The resulting curve closely matches the progression of the MI curve obtained using the conventional evaluation method (red curve). The coefficient of determination, R^2, for both curves was determined to be $R^2 = 0.9925$ [34]. In addition, the blue area represents the force-matched MI curves obtained from 75 linearly increasing measurements. Only the DTIA evaluation window with grip

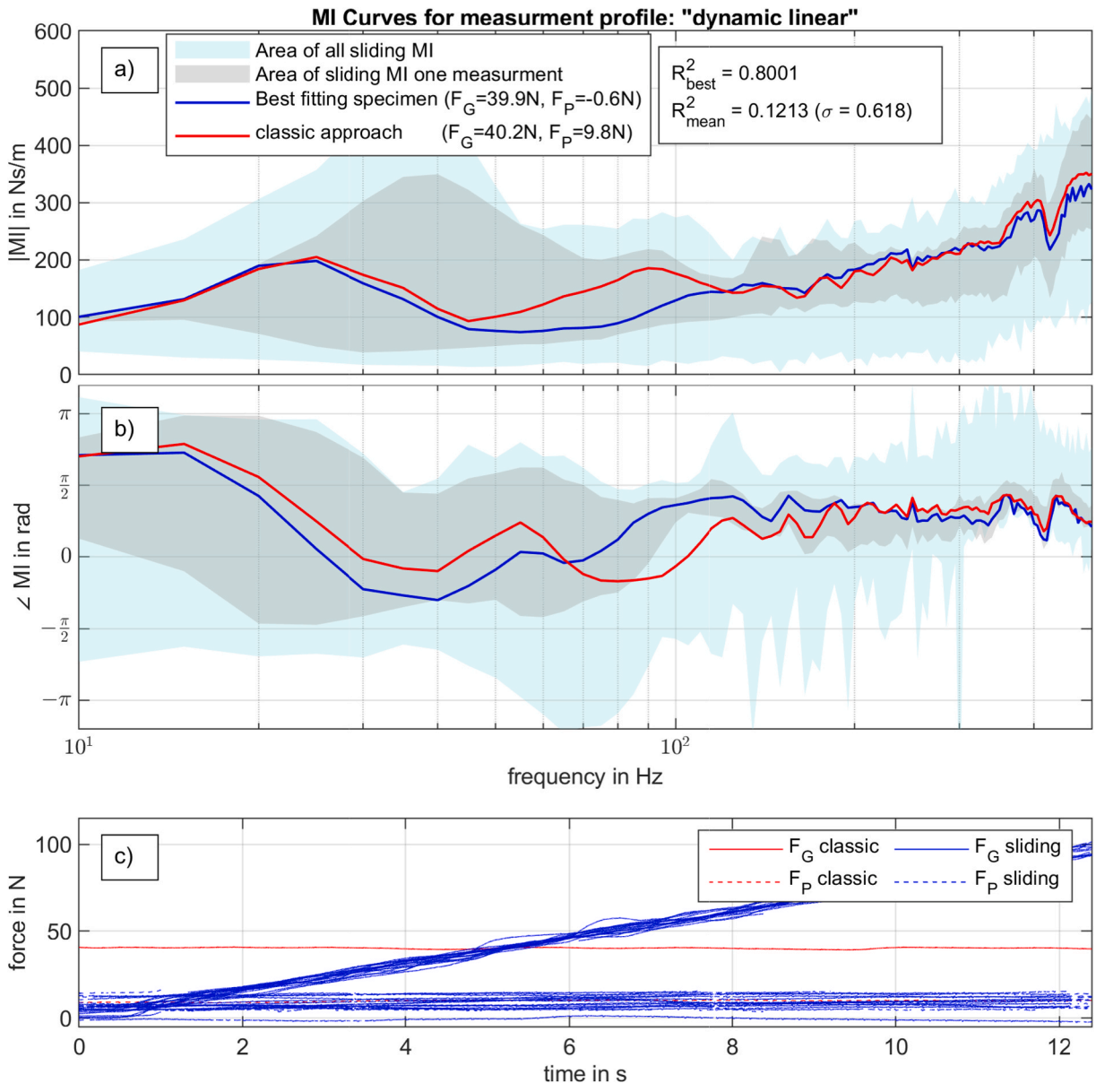


Fig. 6. Top a: 2D display of the mechanical impedance for static forces over a frequency range of 10 to 500 Hz. The mechanical impedance, as determined by the "Reference method", is shown in red and represents the reference [21]. The mechanical impedance curve determined by using the Best Fit approach according to the new method presented in this paper is shown in blue. The correlation between the curves is R^2 of 0.8001..The blue area represents the DTIA results obtained from all 75 linearly increasing dynamic measurements. Across these measurements, the coefficients of determination relative to the static reference had a mean of $Rmean^2 = 0.1213$ with an SD of 0.618. Middle b: The Phase from the mechanical Impedance in rad over the frequency. Bottom c: The grip and push force for static (red) and dynamic (blue) forces in newtons over time.

and push forces closest to the static reference condition was included for each measurement. Across these 75 force-matched comparisons, the mean coefficient of determination relative to the static reference was $R^2_{mean} = 0.6002$, with an SD of 0.351. In comparison the MI values for 2 separate measurements (see Appendix I) that are evaluated with the state-of-the-art method leads to an R2 = 0.9749. The results show that the deviation associated with the new evaluation method is smaller than the variability in repeated measurements from the same individual. This implies that the new method does not introduce any additional variance beyond that naturally present in the participant's measurements.

In the second evaluation step, two different measurements were analysed for the same test subject: a measurement with a constant grip and push force (Formula 1, Static Value), and a measurement with a grip force curve that increased linearly (Formula 2, Linear Value). The static value data sets were processed using the 'reference' evaluation method. For the linear data, the new evaluation method was used. The results are shown in Fig. 6. The lower diagram in Fig. 6 shows the interaction forces over time. For the linear measurement (blue lines), the grip force increases evenly from 0 N to 100 N, while the push force remains approximately 0 N throughout the entire measurement period. The constant measurement is shown in red and exhibits constant grip forces of 40 N as well as constant push forces of 10 N. The upper diagram shows, the MI as a function of frequency. The red curve shows the reference impedance based on the state-of-the-art method with constant interaction forces. The gray area comprises, all MI curves resulting from the new segmentation method. From the total of 63 contained impedance curves, the impedance curve whose force conditions are most similar to the constant reference measurement was identified and is shown as the best fitting specimen as the blue curve. In this case, it corresponds to a segment with interaction forces of 39.9 N grip force

and nearly 0 N push force. Despite the significant differences in interaction force between the reference and dynamic segments, this selected curve shows a high degree of agreement with the red reference curve. The analysis between those two curves yields a coefficient of determination of $R^2 = 0.8001$, confirming a very high degree of agreement between the conventionally determined impedance and the curve determined via dynamic segmentation. The blue area represents the MI curves obtained by applying DTIA to the complete, linearly increasing force profiles of all 75 dynamic measurements from the 25 participants. These curves cover the full range of forces occurring during the measurements. The mean coefficient of determination relative to the red static reference curve across the 75 measurements was $R^2_{mean} = 0.1213$, with an SD of 0.618.

5.2. Dynamic evaluation of mechanical impedance

As described in Section 3, the new method enables an evaluation for dynamic interaction forces. To visualize the influence of the dynamic forces a third axis must be added to the already shown visualizations for MI curves. The following section describes the setup of such a three-dimensional plot in detail. For better understanding, a measurement with constant forces is used to explain how the graphic is set up. Then the same graphic is used with dynamic force behavior. The result is then explained using a dynamic curve of the "linear curve" (Formula 2). The results for the other grip force curves can be found in the appendix II & III.

Fig. 7 shows the classic two-dimensional representation of the MI curves, showing all 63 MI curves in one plot. Each line has a color representing the grip force applied by the participant. This extension makes it possible to recognize the force-dependent dynamics and simultaneously interpret the MI in the context of the current interaction force. In this case, the color-coded representation shows that the grip forces occurring during the measurement under investigation range from 39.6 N to 40.6 N. The integration of force information in the form of a color scale thus increases the informative value of the 2D representation, as changes in impedance can now be directly assigned to the corresponding force levels without having to refer to additional diagrams or tables.

A key result of this work is the introduction of a three-dimensional representation of MI, as shown in Fig. 9. This representation extends the classic two-dimensional analysis (mechanical impedance over frequency) with an additional time axis, showing clearly variation in the impedance during changing grip forces. In addition to the color-coded grip force, the time-based progression of the grip force is integrated as a black line on the right Y-axis, allowing both the force change and the resulting impedance curves to be interpreted simultaneously.

In addition, the MI at a fixed frequency at 70 Hz is shown as a red line over the entire measurement period. The bottom plot shows the MI for 70 Hz as a 2D, time-based line alongside the grip force. This additional projection illustrates that the new 3D representation allows the MI for any frequency to be read as a function of time, even if the underlying coupling forces vary during the experiment.Based on the new three-dimensional representation of MI, an analogous plot can be generated for the time-varying linear force profile ("linear curve") rather than for a static force combination; the resulting visualization is shown in Fig. 8. The segmentation effect is particularly evident, with the dominant influence of changing grip force occurring in the 30–60 Hz range. At the start of the measurement, the participant applies a grip force of approximately 10 N, corresponding to an MI of ~ 50 Ns/m at 50 Hz and a comparatively flat MI-curve profile. Over time, the grip force increases to approximately 110 N after 13 s, yielding an MI of 274.11 Ns/m at 50 Hz and a more undulating MI-curve profile. To further quantify this relationship at a fixed frequency, the bottom subplot depicts grip force (red) and MI at 70 Hz (blue) as functions of time. This plot demonstrates that the approximately linear increase in grip force is accompanied by a pronounced, non-linear increase in MI. This curve is produced because the dynamic method calculates the MI of each combination of grip force and frequency that occurs over time individually. Therefore, the curve

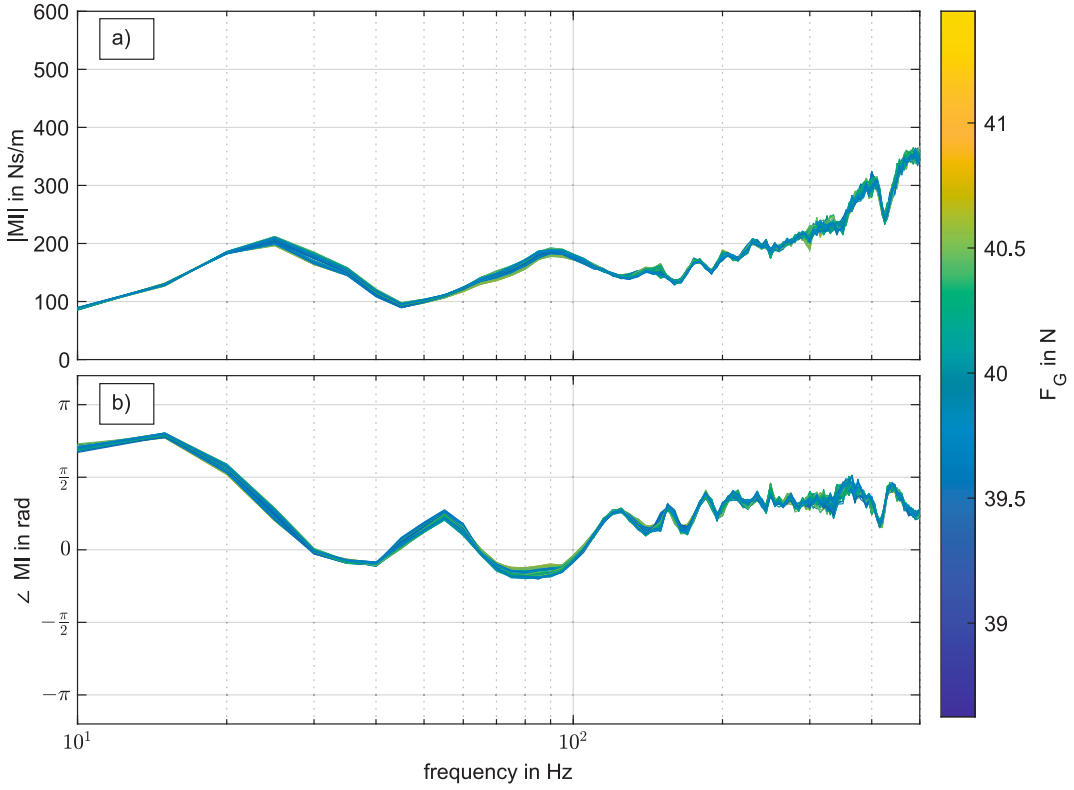


Fig. 7. Top a: Mechanical impedance above a frequency of 10 to 500 Hz, broken down by a color index according to grip force. **Bottom b:** The Phase from the mechanical Impedance in rad over the frequency.

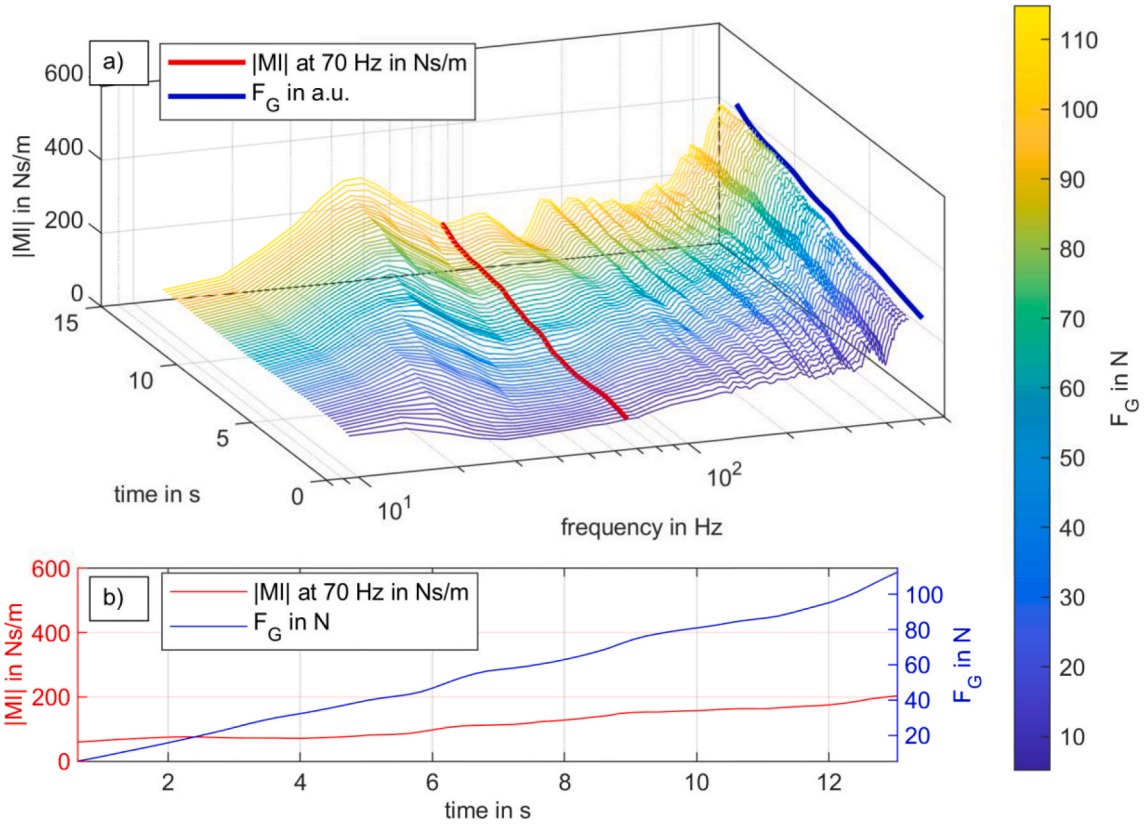


Fig. 8. Top a: 3D graph of the mechanical impedance of a dynamic grip force (linear line in blue) over time (0–15 s) and frequency (10–500 Hz) as a function of grip force (0–110 N)**. Bottom b:** 2D graph: Mechanical impedance at 70 Hz (3D graph as red line) over time with increasing grip force, shown in red.

shown is not the result of a single MI calculation, but rather a combination of many individual, force-specific impedance curves, each of which is valid at the time of its respective measurement.

6. Discussion

This paper presents a new method for evaluating MIs under dynamically varying interaction forces. This approach has been validated using example evaluated using static reference data and 75 dynamic measurements from 25 participants.. In contrast to established methods based on constant force conditions over time Griffin and ISO 10068:2012–12 [12,13], the approach presented here extends the "Reference method". [1,30] by segmenting and overlapping the measurement data. Comparing the conventional static evaluation with the dynamic segmentation method (DTIA) using the same static measured data reveals only minor discrepancies, as evidenced by a high coefficient of determination ($R^2 = 0.9925$). This suggests that, despite using shorter time windows for each segment, the new approach is capable of estimating MI with comparable validity to the established method. The high level of agreement suggests that the essential characteristics of the MI response are preserved even under dynamically varying interaction forces, which demonstrates the robustness of the segmentation-based evaluation. This results in a continuous force-frequency-time connection (see Fig. 4), which allows for a much more differentiated analysis of MI than classic point evaluations. The high correlation between the established and new methods ($R^2 = 0.9925$) confirms the methodological consistency and suitability of the approach for both static and dynamic force conditions [34]. To evaluate consistency between static and dynamic conditions, an impedance curve determined using conventional methods and obtained under a well-defined static force combination was used as a reference. During the dynamic measurement, the segment whose instantaneous force conditions most closely matched those of the static reference was identified. This was possible even though an exact replication of the static force combination could not be achieved due to the continuous nature of the dynamic force progression. The resulting comparison yielded a coefficient of determination of $R^2 = 0.8001$This comparison is notable because the selected dynamic segment closely matched the grip force of the static reference, though not the push force. Therefore, this value should be interpreted as a force approximation rather than evidence of general equivalence between static and dynamic measurements. When DTIA was applied to the full force progression of all 75 dynamic measurements rather than to only the force-matched windows, the mean coefficient of determination relative to the single static reference was found to be $R^2_{mean} = 0.1213$, with an SD of 0.618. This lower level of agreement is expected because the complete DTIA dataset intentionally contains MI curves associated with a broad range of grip force conditions. In contrast, the red reference curve represents a single static interaction force condition. Therefore, the result illustrates the additional force-dependent information retained by DTIA when evaluating the complete dynamic measurement.

How can the dynamic behaviour of mechanical impedance be calculated on varying interaction forces?

Current research shows that vibration transmission and MI are both strongly force-dependent. However, previous studies have only examined this relationship under constant interaction forces [9,14]. Meanwhile, dynamic force curves primarily occur in real-world applications [3,17]. The results of this study confirm the existing understanding that MI increases with rising grip force in a distinctly non-linear manner, as illustrated in Fig. 8. This non-linearity aligns with prior research and can be attributed to alterations in muscle activation, joint stiffness, and soft-tissue compression at varying force levels, each of which modifies the biodynamic response of the hand-arm system. The new method provides an approach that can map these time-varying forces and determine the corresponding MI for the first time. Additionally, this method

significantly reduces experimental effort because a single dynamic measurement captures a large number of force combinations [10,18].

The novelty of DTIA does not lie in the individual signal-processing operations of segmentation and overlapping-window analysis. Rather, it lies in integrating these established operations with the frequency-domain mechanical-impedance calculation to obtain a sequence of force-associated impedance spectra during a single continuous measurement. Evaluated data show that MI increases nonlinearly with increasing gripping force [21,24]. This finding is particularly relevant within the typical tool frequency range of 30–80 Hz because it directly impacts the development of handheld tools [35]. The 2D color-coded grip force representation introduced in this study significantly improves the interpretability of force-dependent impedance phenomena. The broad distribution of the measured MI and phase responses is likely influenced by multiple factors, including anthropometric differences between subjects and variations in hand-handle coupling conditions. Since no target push force was specified during the measurements, subject-specific differences in the applied push force may also have contributed to the observed scatter of the results. Likewise, the phase response should be interpreted in the context of interaction-force conditions. Previous measurements using the established configuration revealed force-dependent changes in MI phase, especially at lower frequencies for grip force changes and within specific frequency ranges for push force changes [29]. Therefore, deviations in phase cannot be attributed to the DTIA evaluation. The DTIA does not modify the underlying force and acceleration measurement chain, but rather applies a time-resolved evaluation to these established signals.

Extending this to a 3D representation offers a significant functional advantage: MI can be read directly over time for each frequency. This is a decisive step toward realistic evaluations of nonstationary force conditions [36]. Displaying individual frequency components, like the example shown in Fig. 9, as independent time-dependent curves achieves a level of understanding not yet seen in the literature. This improvement is made possible by combining segmentation and overlap according to Welch's principle [29].

More broadly, the presented method opens new perspectives for the ergonomic evaluation and risk assessment of hand-arm vibrations. Because it can realistically represent dynamic impedance curves, this method could be integrated into future HAV assessment standardization, complementing existing standards such as ISO 10068:2012–12 [13]. With a more comprehensive database, the method could also be used to develop a complete force–time-frequency model of the hand-arm system. This could lay the groundwork for future biodynamic hand-arm models and the design of vibration-optimized tools.

7. Limitation

The study was conducted using sample measurement data from 25 test subjects for linear time varying curve and two test subjects for static curve. This small sample size may have led to irregularities in the measurement data. However, even if such irregularities did occur, they are not relevant for this study, since the objective is to prove the validity of the newly developed measurement method and to show that it can also be used to evaluate dynamic grip forces. The measurements were carried out with a limited number of test subjects and exemplary force curves. Thus, no generalizable biomechanical parameters can be derived. To solve this problem, future studies should therefore extend to larger samples and consider realistic nonlinear interaction forces [17]. A limitation of the present study is that push force was not controlled as an independent experimental variable. Similar to the procedure reported

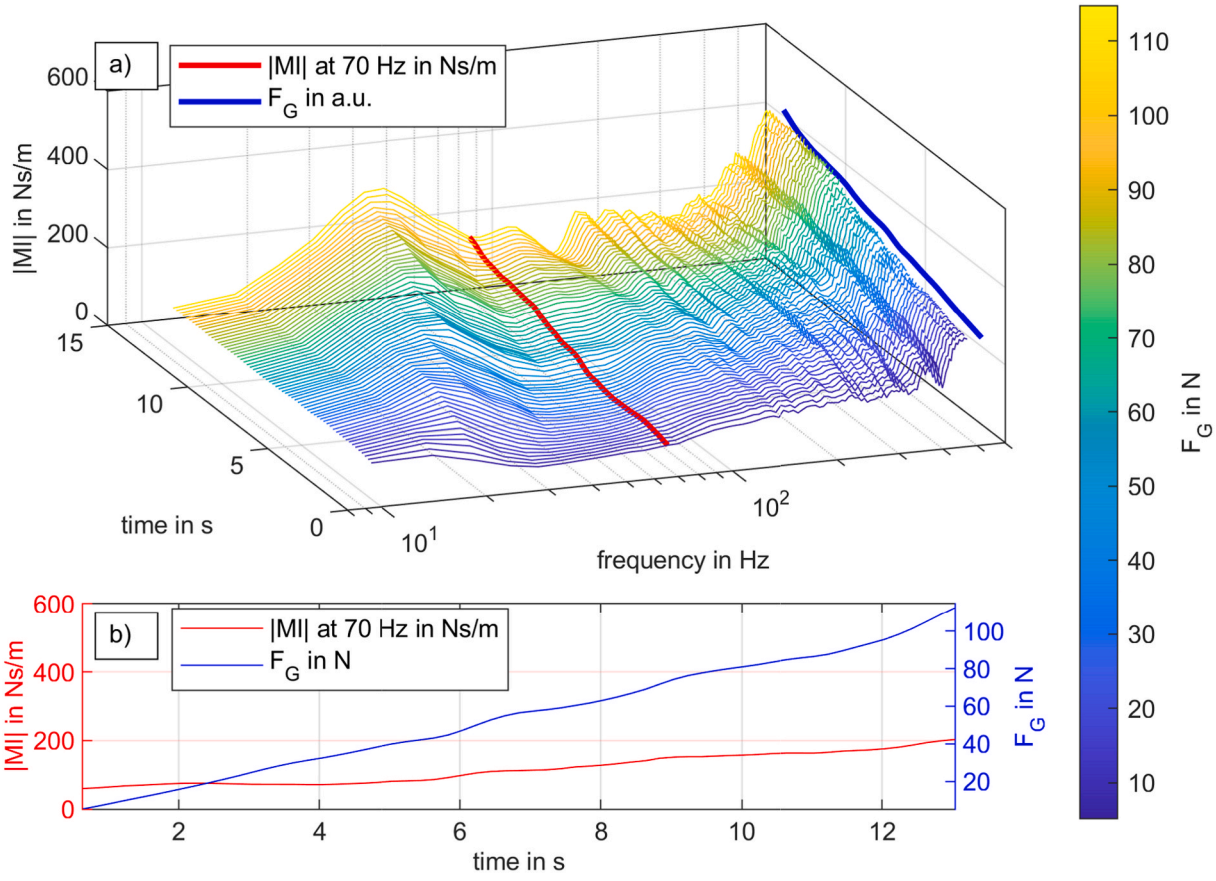


Fig. 9. Top a: 3D graph of the mechanical impedance of a quasi-static grip force (constant value) over time (0–15 s) and frequency (10–500 Hz) as a function of the grip force (approx. 40 N). **Bottom b:** 2D curve of the mechanical impedance for 70 Hz of a quasi-static grip force in Newton (constant value approx. 40 N) over time.

by Pan et al. [25], only the grip force was continuously varied. Therefore, differences in the naturally applied push force between subjects may have introduced additional variability into the measured biodynamic responses. Previous research has reported significant variability among individuals in hand-arm muscle injury and has discussed anthropometric characteristics as a possible contributing factor [30]. However, the present study was not designed to quantify the influence of these parameters. Additionally, existing studies highlight the importance of different grip positions and realistic tool interfaces [16,20]. Further studies should investigate these as well.

The accuracy of the new method depends on the sampling rate and the accuracy of the test bench. A higher sampling rate can provide more accurate and meaningful data. Furthermore, this could allow for a finer segmentation, while keeping the same frequency resolution. This would also probably increase the significance of the individual MI curves. The conducted measurements are sampled with 10 kHz which leads to a frequency resolution of 0.1 Hz per second measuring time. In combination with the used frequency step of 5 Hz for the multi-sine a segmentation into smaller samples is not suitable. However, this problem can be solved by using a higher sampling rate in combination with fitting sensors.

8. Conclusion

This paper presents a new method, DTIA-Dynamic Time-Resolved MI Analysis, for evaluation MI under dynamic interaction forces, and validates it, while established methods are based on static, time-constant force levels. The presented method enables, for the first time, a continuous and time-resolved analysis of MI under varying coupling forces. To this end, the data are segmented and processed using overlapping windows. This allows the MI to be represented as a time-resolved curve across the dynamic force conditions and frequencies present during the experiment.

A comparison with the established static evaluation method shows that the new DTIA-method delivers almost identical results for constant force conditions. This confirms the methodological validity for the static case. At the same time, dynamic evaluation opens the possibility of reliably determining MI even for time-based variable interaction forces. This is an aspect that was not previously possible. The application to 75 dynamic measurements from 25 participants further demonstrates that force-specific MI curves can be extracted from continuously varying measurements. This capability is particularly relevant because real human–machine interactions, such as with hand-held tools, are primarily characterized by dynamic force curves.

The measurements performed are from exemplary nature and were not carried out with the objective of deriving definitive biomechanical parameters for the hand-arm system. Rather, they serve to test the functionality and consistency of the developed evaluation method. The results clearly show that the DTIA-method presented forms a viable basis for future studies with realistic dynamic force curves. A key practical advantage of the new method is that extensive measurement series with numerous static repetitions will no longer be necessary in the future. Instead, a wide range of force-frequency combinations can be derived from a single dynamic measurement and their influence on MI analyzed. This not only significantly shortens measurement times but also increases the informative value of experimental investigations under realistic conditions.

Overall, this method is a significant step toward more realistic and efficient characterization of the hand-arm system. It also opens new possibilities for investigating vibration loads under dynamic interaction forces. The principle of determining MI as a time-resolved function of dynamic coupling forces, which is used in hand-arm applications, may also be applicable to other human-vibration scenarios. Examples include whole-body vibration when standing on vibrating platforms or when seated in vehicles, where vibrations are transmitted through the seat interface. In these cases, the method could be adapted by replacing grip force with the relevant coupling forces acting at the feet, pelvis or back.

Declaration of Generative AI use in the writing process

The authors used Deepl SE, Copilot and ChatGPT5.2 to improve writing and language skills and subsequently reviewed and edited all content, assuming full responsibility for the publication.

CRediT authorship contribution statement

Saurbier Simon: Writing – original draft, Visualization, Validation, Software, Methodology, Investigation, Formal analysis, Data curation, Conceptualization. **Wolter Kai:** Writing – review & editing, Visualization, Validation, Software, Methodology, Investigation, Formal analysis. **Spengler Carina:** Software, Methodology, Formal analysis, Data curation. **Bunk Lukas:** Writing – review & editing, Methodology. **Jan-Heinrich Robens:** Writing – review & editing. **Krause Dieter:** Supervision. **Matthiesen Sven:** Writing – review & editing, Supervision, Resources.

Declaration of competing interest

The authors declare that they have no known competing financial interests or personal relationships that could have appeared to influence the work reported in this paper.

Acknowledgement

This research is funded by the German Research Foundation (DFG) under proposals 530564503 ('Dynamically adaptive impedance elements for influencing vibrations in validation environments'). The test equipment has been supported accordingly DFG (275571425). The authors bear sole responsibility for the research results, which do not represent the official opinion of the DFG.

I Appendix. – Mechanical impedance for two separate measurements was calculated using a reference method

I. Appendix – Mechanical impedance for two separate measurements was calculated using a reference method

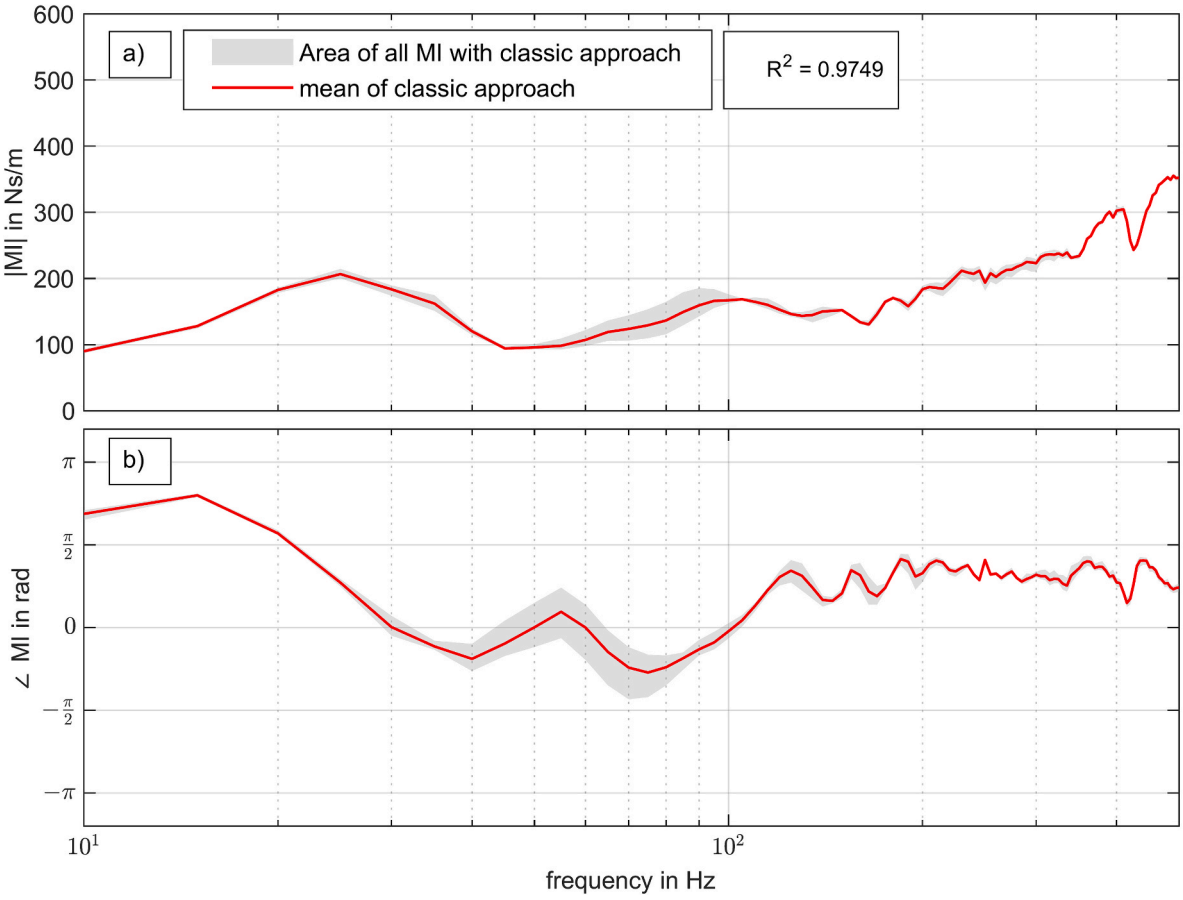


Fig. 10. ***Top a:*** *The dispersion within an evaluation of the mechanical impedance curve is shown in gray as an area and in red as a mean value.* ***Bottom b:*** *The Phase from the mechanical Impedance in rad over the frequency.*

II Appendix. – Mechanical impedance (Example: Test subject 1)

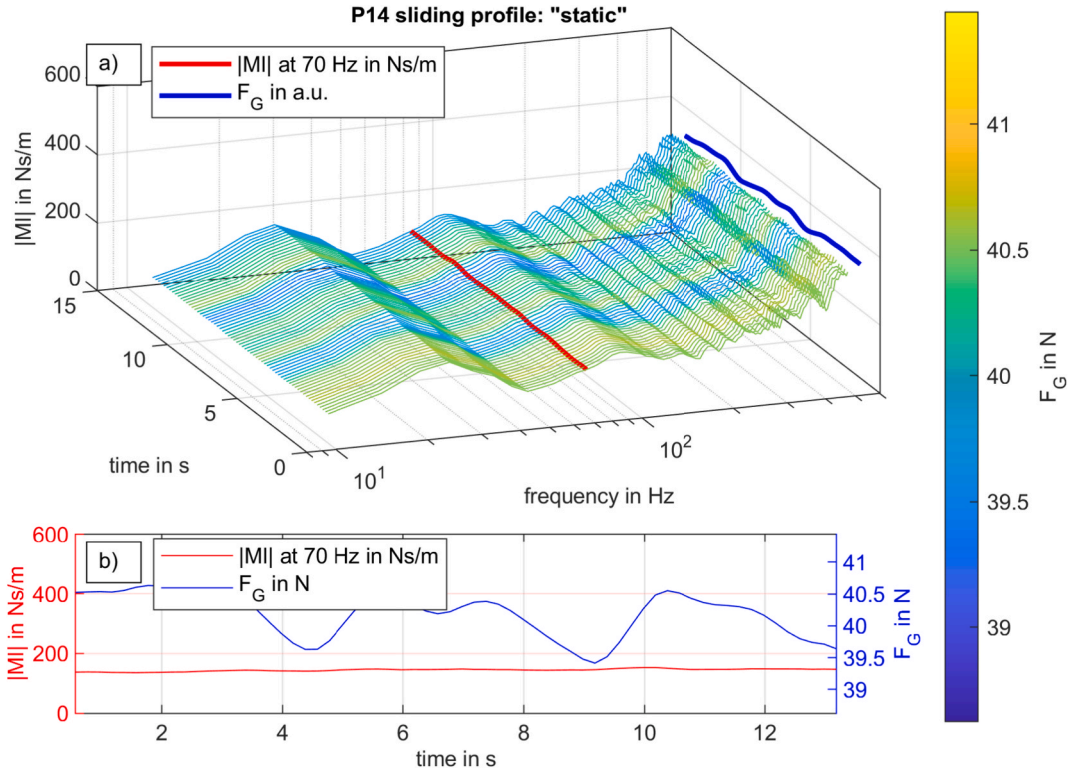


Fig. 11. Top a: 3D graph of the mechanical impedance for subject 1 of a quasi-static grip force (constant value) over time (015 s) and frequency (10500 Hz) as a function of the grip force (approx. 40 N). **Bottom b:** 2D curve of the mechanical impedance for 70 Hz of a quasi-static grip force in Newton (constant value approx. 40 N) over time.

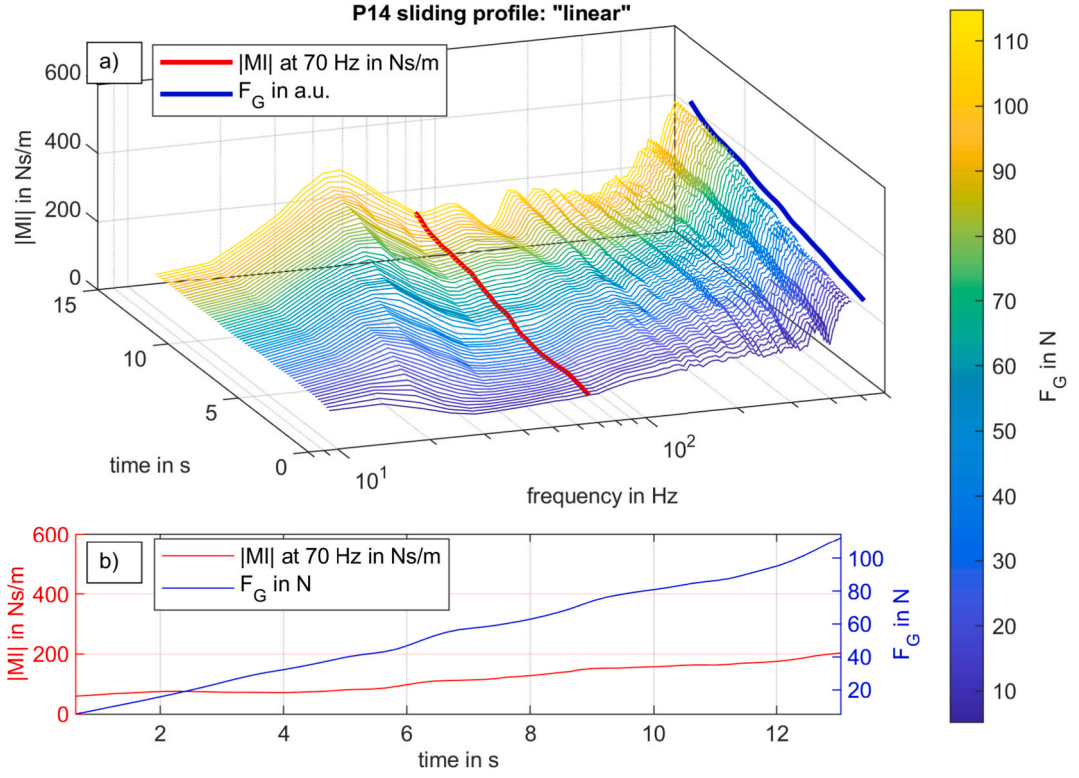


Fig. 12. Top a: 3D graph showing the mechanical impedance of subject 1 for a linear grip force over time (0–15 s) and frequency (10–500 Hz). **Bottom b:** 2D curve showing the mechanical impedance at 70 Hz as a function of grip force in Newtons over time.

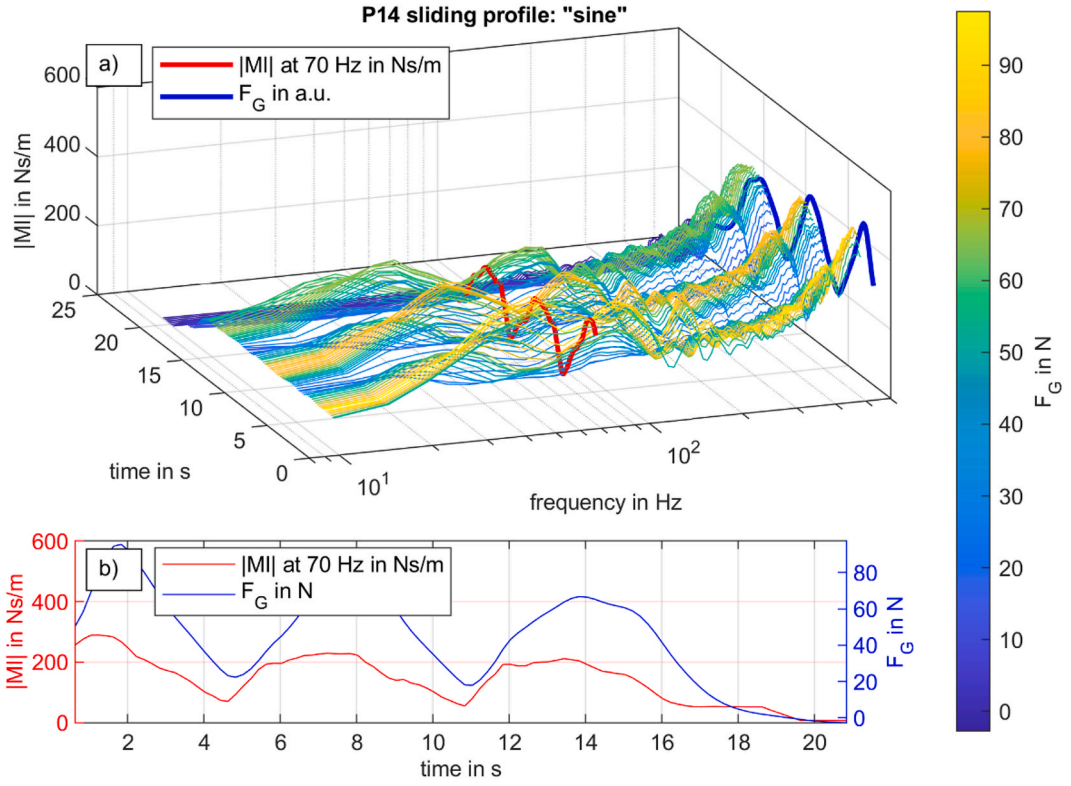


Fig. 13. Top a: 3D graph showing the mechanical impedance of subject 1 as a function of grip force (sine curve), frequency (10–500 Hz) and time (0–15 s). **Bottom b**: 2D curve showing the mechanical impedance of a 70 Hz sine curve grip force in Newtons over time.

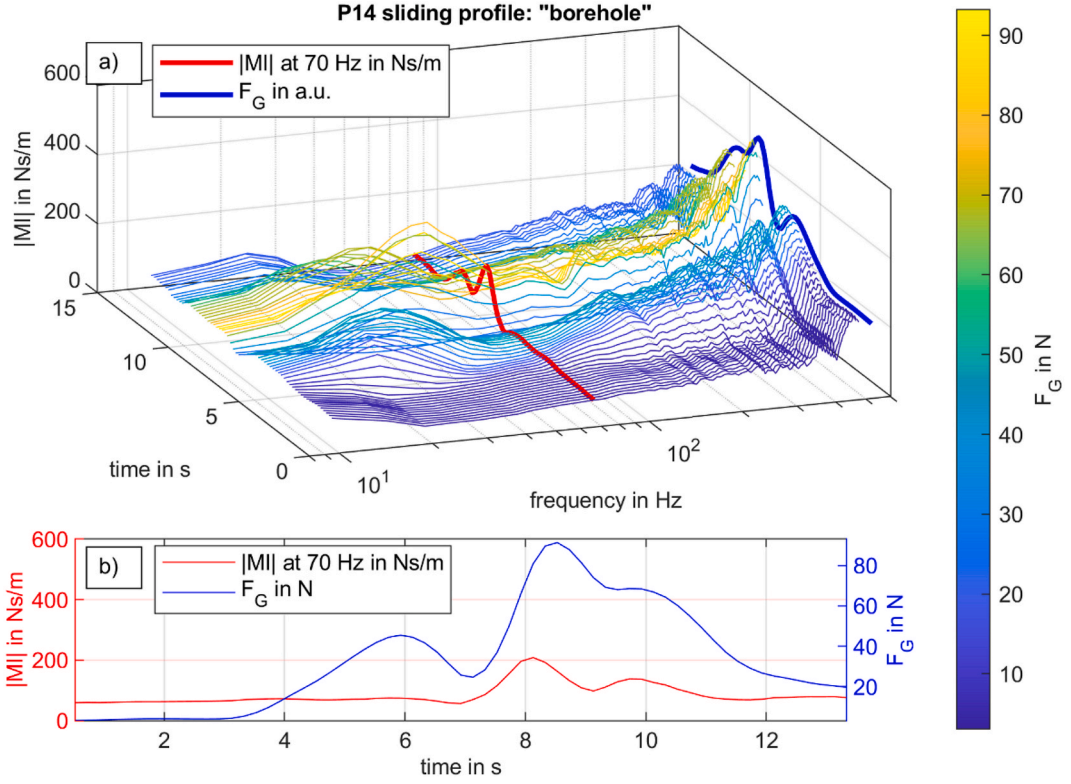


Fig. 14. Top a: 3D graph showing the mechanical impedance of subject 1′s hammer drilling grip force curve over time (0–15 s) and frequency (10–500 Hz). **Bottom b:** 2D curve showing the mechanical impedance at 70 Hz of a hammer drilling grip force curve in Newtons over time.

III Appendix. – Mechanical impedance (Example: Test subject 2)

I. Appendix – Mechanical Impedance (Example: Test Subject 2):

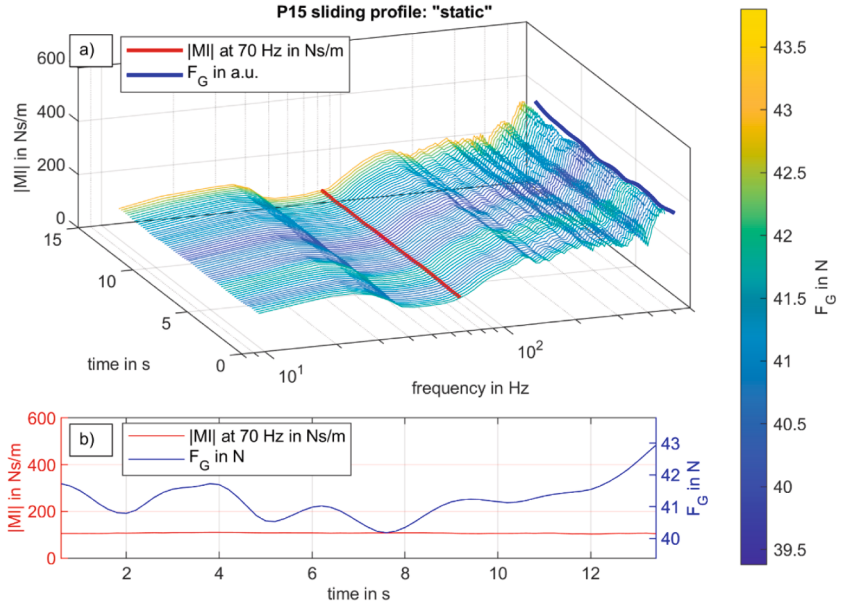


Fig. 15. Top a: 3D graph of the mechanical impedance for subject 2 of a quasi-static grip force (constant value) over time (015 s) and frequency (10500 Hz) as a function of the grip force (approx. 40 N). **Bottom b:** 2D curve of the mechanical impedance for 70 Hz of a quasi-static grip force in Newton (constant value approx. 40 N) over time.

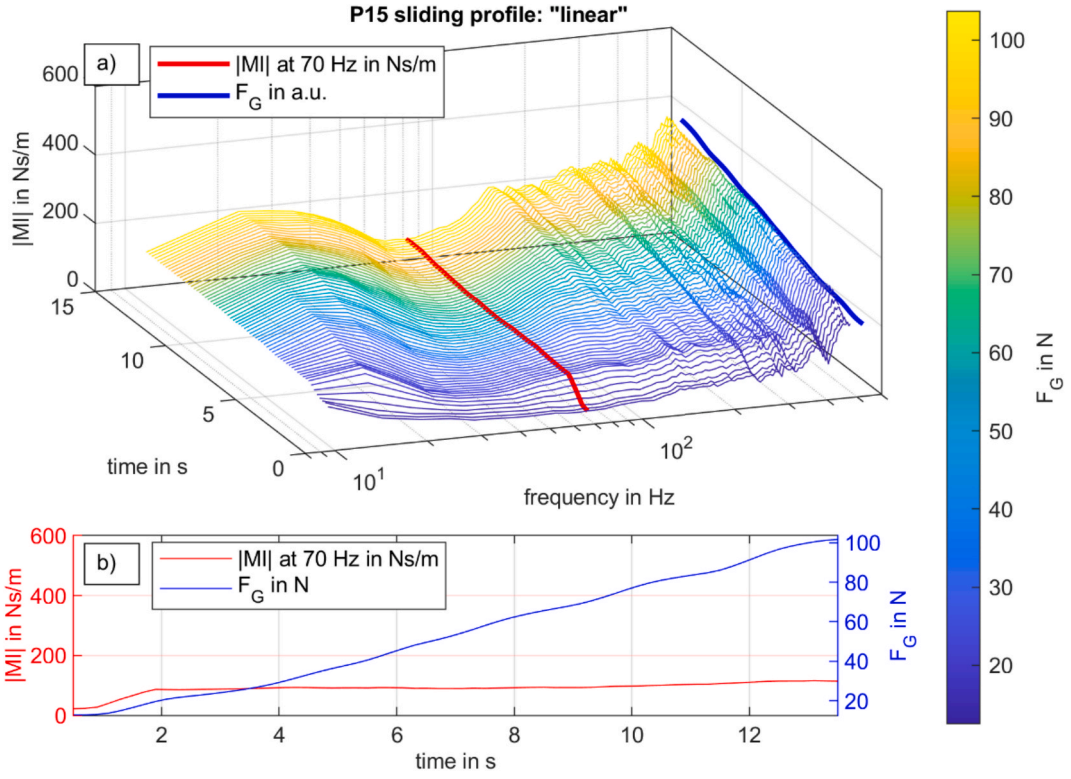


Fig. 16. Top a: 3D graph showing the mechanical impedance of subject 2 for a linear grip force over time (0–15 s) and frequency (10–500 Hz). **Bottom b:** 2D curve showing the mechanical impedance at 70 Hz as a function of grip force in Newtons over time.

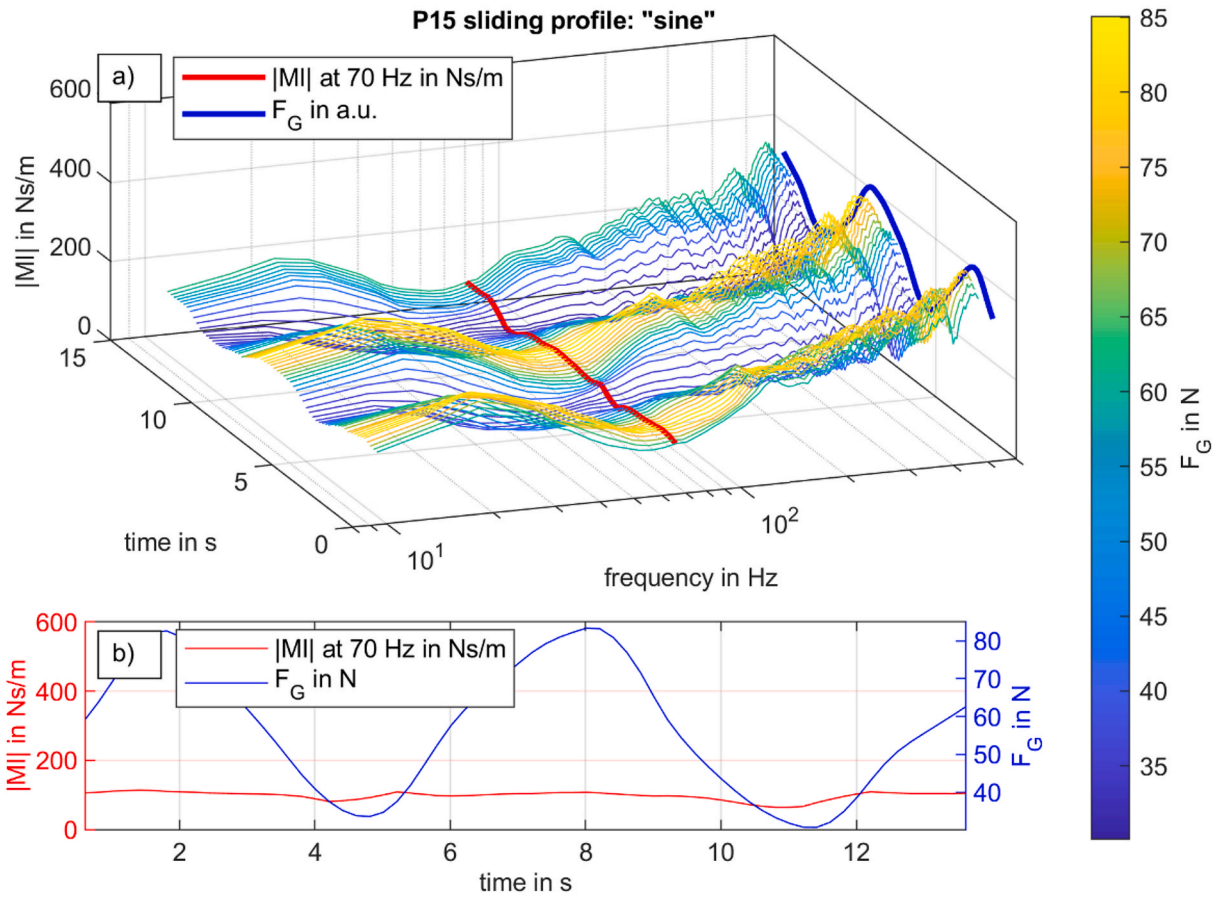


Fig. 17. **Top a:** 3D graph showing the mechanical impedance of subject 2 as a function of grip force (sine curve), frequency (10–500 Hz) and time (0–15 s). **Bottom b**: 2D curve showing the mechanical impedance of a 70 Hz sine curve grip force in Newtons over time.

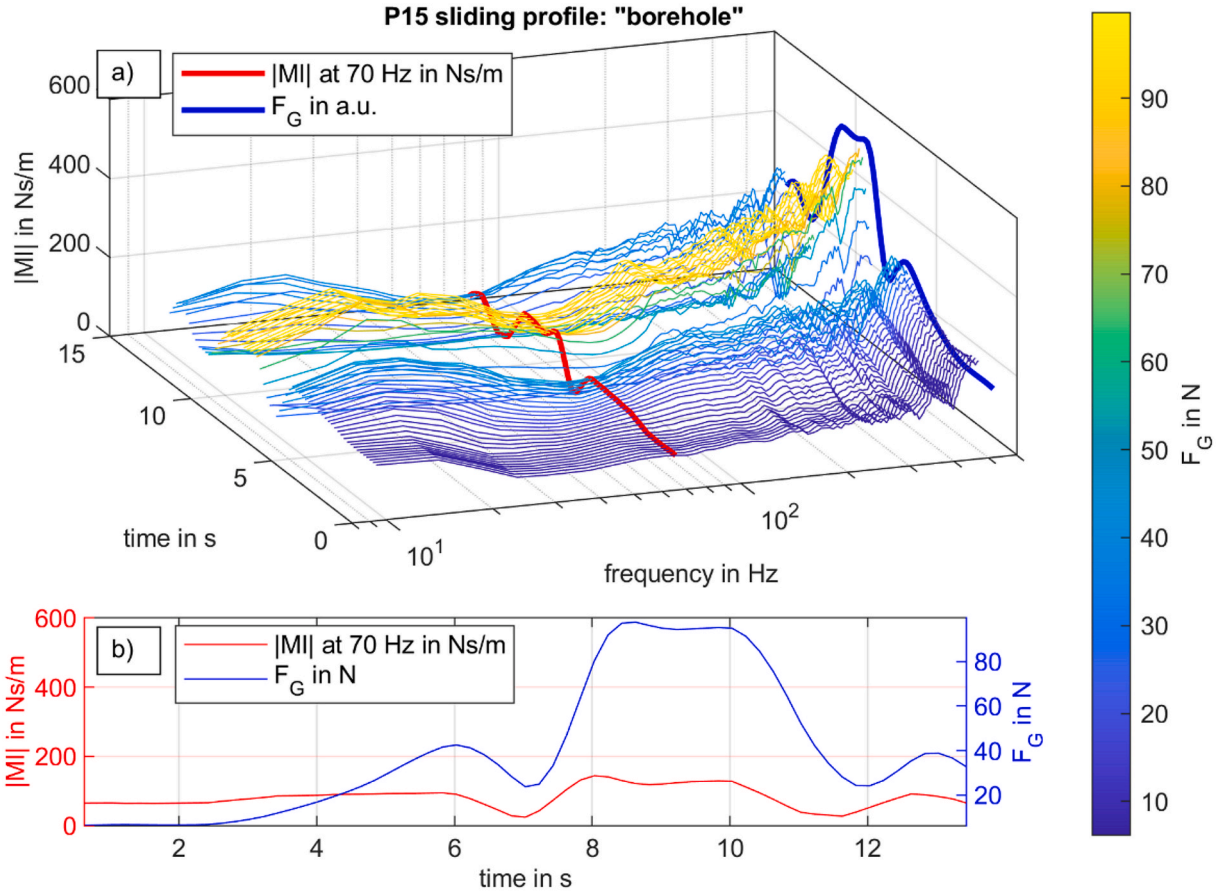


Fig. 18. Top a: 3D graph showing the mechanical impedance of subject 2's hammer drilling grip force curve over time (0–15 s) and frequency (10–500 Hz). **Bottom b:** 2D curve showing the mechanical impedance at 70 Hz of a hammer drilling grip force curve in Newtons over time.

Data availability

Data will be made available on request.

References

[1] A. Lindenmann, M. Uhl, T. Gwosch, et al., The influence of human interaction on the vibration of hand-held human-machine systems - the effect of body posture, feed force, and gripping forces on the vibration of hammer drills, Appl. Ergon. 95 (2021) 103430, https://doi.org/10.1016/j.apergo.2021.103430.

[2] D.D. Reynolds, E.N. Angevine, Hand-arm vibration, part II: vibration transmission characteristics of the hand and arm, J. Sound Vib. 51 (1977) 255–265, https://doi.org/10.1016/S0022-460X(77)80035-7.

[3] A.F. Cristea, M.C. Bălcău, S. Haragâș, A Chronological Review of the Transmission and Effects of Mechanical Vibrations on the Hand—Arm System in an Occupational Workplace, Appl. Sci. 15 (2025) 1182, https://doi.org/10.3390/app15031182.

[4] E. Greenslade, T.J. Larsson, Reducing vibration exposure from hand-held grinding, sanding and polishing powertools by improvement in equipment and industrial processes, Saf. Sci. 25 (1997) 143–152, https://doi.org/10.1016/S0925-7535(97)00040-4.

[5] (2019) Directive 2002/44/EC of the European Parliament and of the Council of 25 June 2002 on the minimum health and safety requirements regarding the exposure of workers to the risks arising from physical agents (vibration) (sixteenth individual Directive within the meaning of Article 16(1) of Directive 89/391/EEC) - Joint Statement by the European Parliament and the Council: 32002L0044.

[6] B. Halmai, T.P. Holsgrove, S.J. Vine, et al., The after-effects of occupational whole-body vibration on human cognitive, visual, and motor function: a systematic review, Appl. Ergon. 118 (2024) 104264, https://doi.org/10.1016/j.apergo.2024.104264.

[7] J.Z. Wu, R.G. Dong, D.E. Welcome, et al., A method for analyzing vibration power absorption density in human fingertip, J. Sound Vib. 329 (2010) 5600–5614, https://doi.org/10.1016/j.jsv.2010.07.022.

[8] S. Adewusi, S. Rakheja, P. Marcotte, et al., Distributed vibration power absorption of the human hand-arm system in different postures coupled with vibrating handle and power tools, Int. J. Ind. Ergon. 43 (2013) 363–374, https://doi.org/10.1016/j.ergon.2013.04.004.

[9] R.G. Dong, J.Z. Wu, D.E. Welcome, et al., Estimation of vibration power absorption density in human fingers, J. Biomech. Eng. 127 (2005) 849–856, https://doi.org/10.1115/1.1992526.

[10] Spengler C, Saurbier S, Lindenmann A et al. (2026) Modeling the Influence of Grip and Push Force Variations on the Mechanical Impedance and Vibration Power Absorption of the Hand-Arm System. https://doi.org/10.1016/j.rineng.2026.113151.

[11] Deutsches Institut für Normung, DIN EN ISO 22867, Forst- und Gartenmaschinen - Schwingungsmessnorm für handgehaltene Maschinen mit Verbrennungsmotor - Schwingungen an den Handgriffen (ISO 22867:2021): = Forestry and gardening machinery - vibration test code for portable hand-held machines with internal combustion engine - vibration at the handles (ISO 22867:2021), Deutsche Fassung EN ISO 22867:2021, Beuth Verlag GmbH, Berlin, Deutsche Norm, 2022.

[12] M.J. Griffin, Handbook of human vibration, Academic Press, London, 1990.

[13] ISO International Standard (2012) ISO 10068:2012-12: Mechanical vibration and shock - Mechanical impedance of the human hand-arm system at the driving point 13.160(10068:2012-12).

[14] S.A. Adewusi, S. Rakheja, P. Marcotte, et al., Vibration transmissibility characteristics of the human hand–arm system under different postures, hand forces and excitation levels, J. Sound Vib. 329 (2010) 2953–2971, https://doi.org/10.1016/j.jsv.2010.02.001.

[15] J.M. Dolan, M.B. Friedman, M.L. Nagurka, Dynamic and loaded impedance components in the maintenance of human arm posture. IEEE Trans Syst, Man, Cybern 23 (1993) 698–709, https://doi.org/10.1109/21.256543.

[16] J.-H. Lin, R.W. McGorry, C.-C. Chang, Hand-handle interface force and torque measurement system for pneumatic assembly tool operations: suggested enhancement to ISO 6544, J. Occup. Environ. Hyg. 4 (2007) 332–340, https://doi.org/10.1080/15459620701285644.

[17] Saurbier, S., Pisarzowski, M., Becker, A., Kleinhans, L., Bunk, L., Krause, D., Matthiesen, S. (2026). Measurement and Evaluation of the Interaction Forces of Specific Hammer Drilling Strategies to Determine Requirements for Dynamic Hand-Arm Models. In: Isabel L. Nunes (eds) Human Factors and Systems Interaction. AHFE (2026) International Conference. AHFE Open Access, vol 230. AHFE International, USA. https://doi.org/10.54941/ahfe1007978.

[18] Jahn R (1985) Einflußgrößen auf die Beschleunigungen elektropneumatischer Bohrhämmer. Dissertation, Universität Dortmund.

[19] M. Uhl, T. Bruchmüller, S. Matthiesen, Experimental analysis of user forces by test bench and manual hammer drill experiments with regard to vibrations and

productivity, Int. J. Ind. Ergon. 72 (2019) 398–407, https://doi.org/10.1016/j.ergon.2019.06.016.
[20] D. Welcome, S. Rakheja, R. Dong, et al., An investigation on the relationship between grip, push and contact forces applied to a tool handle, Int. J. Ind. Ergon. 34 (2004) 507–518, https://doi.org/10.1016/j.ergon.2004.06.005.
[21] P. Forte, Identification of the hand-arm system mechanical impedance by simultaneous measurement of grip, transmitted force and acceleration with an adaptable instrumented handle, Cogent Eng. 4 (2017) 1291778, https://doi.org/10.1080/23311916.2017.1291778.
[22] Y. Aldien, P. Marcotte, S. Rakheja, et al., Influence of hand forces and handle size on power absorption of the human hand–arm exposed to zh-axis vibration, J. Sound Vib. 290 (2006) 1015–1039, https://doi.org/10.1016/j.jsv.2005.05.005.
[23] S. Aatola, Transmission of vibration to the wrist and comparison of frequency response function estimators, J. Sound Vib. 131 (1989) 497–507, https://doi.org/10.1016/0022-460X(89)91009-2.
[24] R. Oddo, T. Loyau, P.E. Boileau, et al., Design of a suspended handle to attenuate rock drill hand-arm vibration: model development and validation, J. Sound Vib. 275 (2004) 623–640, https://doi.org/10.1016/j.jsv.2003.06.006.
[25] D. Pan, X.S. Xu, D.E. Welcome, et al., The relationships between hand coupling force and vibration biodynamic responses of the hand-arm system, Ergonomics 61 (2018) 818–830, https://doi.org/10.1080/00140139.2017.1398843.
[26] Deutsches Institut für Normung (2021) Mechanische Schwingungen und Stöße - Hand-Arm-Schwingungen - Messung und Bewertung der Schwingungsübertragung von Handschuhen in der Handfläche (ISO 10819:2013 + Amd.1:2021): Mechanical vibration and shock - Hand-arm vibration - Measurement and evaluation of the vibration transmissibility of gloves at the palm of the hand 13.160(10819:2021).
[27] E. Heyden, A. Lindenmann, S. Matthiesen, et al., Approach for calibrated measurement of the frequency response for characterization of compliant interface elements on vibration test benches, Appl. Sci. 11 (2021) 9604, https://doi.org/10.3390/app11209604.
[28] H. Fu, Y. Yu, Y. Chen, et al., Direct measurement for hand-transmitted vibration of human fingers-hand-arm system in the zero-gravity environment, Adv. Space Res. 74 (2024) 3916–3924, https://doi.org/10.1016/j.asr.2024.06.062.
[29] P. Welch, The use of fast Fourier transform for the estimation of power spectra: a method based on time averaging over short, modified periodograms, IEEE Trans. Audio Electroacoust. 15 (1967) 70–73, https://doi.org/10.1109/TAU.1967.1161901.
[30] A. Lindenmann, T. Schröder, R. Germann, et al., Effect of high level grip-and push force and elevated arm posture on the zh-axis hand-arm impedance, Int. J. Ind. Ergon. 92 (2022) 103375, https://doi.org/10.1016/j.ergon.2022.103375.
[31] R.G. Dong, D.E. Welcome, T.W. McDowell, et al., Measurement of biodynamic response of human hand–arm system, J. Sound Vib. 294 (2006) 807–827, https://doi.org/10.1016/j.jsv.2005.12.047.
[32] Saurbier S, Spengler C, Kienzle J et al. (2025) Modeling realistic grip force curves from hammer drill applications to determine mechanical impedance using a translational shaker system. In: VDI Wissensforum GmbH (ed) 5. VDI-Fachtagung Schwingungen 2025, 5th edn., VDI Berichte 2463. VDI Verlag GmbH, Düsseldorf, pp 229–242. https://doi.org/10.51202/9783181024638-229.
[33] DIN Deutsches Institut für Normung e.V. (2001) DIN EN ISO 5349 Messung und Bewertung der Einwirkung von Schwingungen auf das Hand-Arm-System des Menschen - Teil 1: Allgemeine Anforderungen.
[34] N.R. Draper, H. Smith, Applied Regression Analysis, Wiley, 1998.
[35] S. Matthiesen, S. Mangold, T. Bruchmueller, The influence of variating passive user interactions on power tools in the context of product development, Forsch. Ingenieurwes. 82 (2018) 157–168, https://doi.org/10.1007/s10010-018-0269-x.
[36] A. Oppenheim, R. Schafer, Discrete-Time Signal Processing: Pearson New International Edition, 3. Auflage, Pearson Education Limited, Harlow, 2013.